

A NEW RFQ MODEL APPLIED TO THE ESTIMATION OF MECHANICAL DEFAULTS DISTRIBUTION

François SIMOENS[†], Alain FRANCE, Jacques GAIFFIER,
CEA SACLAY, 91191 Gif-sur-Yvette, FRANCE

Abstract

As part of the High Intensity Proton Injector project (IPHI), a 6 meters-long aluminum RFQ cold model has been built. This prototype is designed to elaborate the RF tuning procedures that will be applied at several steps of the final cavity machining and assembly. This study has implied the building of a complete theoretical modelization of RFQs. The analysis of the measurements with our formalism can generate slug tuners commands or capacitances defaults. These capacitances defaults are transformed into estimation of the longitudinal distribution of the mechanical disequilibria between the quadrants of the RFQ whatever the boundary conditions are. We present the tests that we made to verify the relation between the mechanical defaults and the estimated electrical errors.

1 INTRODUCTION

The development of our complete formalism has led to the conception of a new RF diagnosis of the mechanical defaults. Expressed as deviations of the capacitances of a perfectly symmetrical RFQ, these RF estimations are related to the mechanical disequilibria of the central region delimited by vane tips. This paper shows tests realized on our RFQ cold-model that validate this new experimental tool.

2 MECHANICAL DEFAULTS RF DIAGNOSIS

The IPHI RFQ study has implied the build-up of a complete theoretical formalism [1].

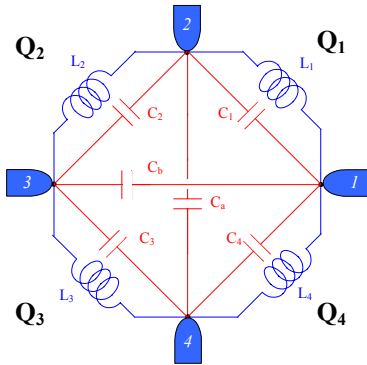


Fig. 1: equivalent circuit shunt elements

The central region delimited by electrode tips is modeled by an inhomogeneous 4-wire line system. The

parallel lumped elements of the equivalent circuit (Fig. 1) are:

- A shunt L_i, C_i resonant circuit corresponding to the i -th quadrant Q_i .
- Capacitances C_a and C_b coupling opposite electrodes.

In a perfectly symmetrical RFQ, for $i=1\dots 4$, $C_i=C$, $L_i=L$, $C_a=C_b$.

2.1 Capacitances default estimation

The 4 voltages between electrodes are solution of a vector eigen-value problem whose differential operator M is derived from the 4-wire line equations. The first order perturbation of M is expressed as combination of small variations of dL_i, dC_i, dC_a and dC_b . Since the dimension of the vector problem is only 3, these 10 functions of abscissa cannot be recovered from a single bead-pull measurement. For a measured quadrupolar mode, theoretical analysis [1] shows that following capacitance defaults may be extracted:

$$dC_{Q0} = (dC_1 + dC_2 + dC_3 + dC_4) / 4$$

$$dC_{SQ} = (dC_1 - dC_3) / 2$$

$$C_{TQ} = (dC_4 - dC_2) / 2$$

These three parameters are respectively expanded on NQ, NS and NT eigen-modes, with the following limitations:

- The number of discrete points chosen between mechanical irregularities within the measured H-field profile.
- The signal to noise ratio that becomes critical for higher orders modes.

A fourth parameter is also extracted from the (possibly) separated dipolar resonance frequencies:

$$dC_{SST} = dC_1 + dC_2 - dC_3 - dC_4$$

with the fundamental component only available.

From these 4 quantities, each quadrant dC_i is computed.

2.2 End boundary independence

End boundary conditions are extracted from the measured fields before expansion. So the measured fields are projected on a eigen-base corresponding to the ideal RFQ with the real RFQ end regions tuning. That way the capacitances of the central region are estimated whatever the boundary conditions are.

[†]fsmoens@cea.fr

3 VALIDATION OF THE RELATION BETWEEN MECHANICAL DEFAULT AND RF DIAGNOSIS

3.1 RFQ cold-model specific conception

Up to 6 segments can be assembled in many configurations. The removable vanes are screwed in 1-m long bodies.

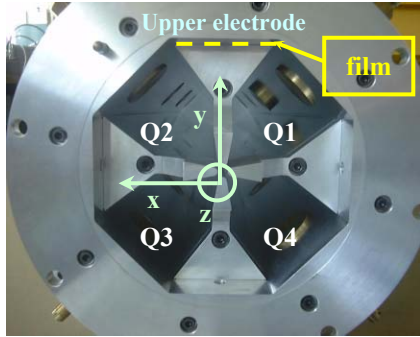
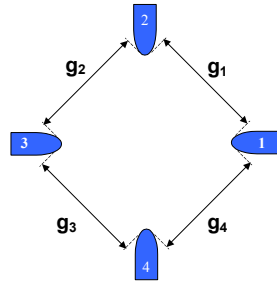


Fig. 2: RFQ cold-model transverse section

Two of these bodies have octagonal transverse section where the upper electrodes (Fig. 2) can be mechanically displaced:

- Horizontally by gliding the vane on the octagon basis.
- Vertically by removing the 0,1 mm thick copper film that is by-default inserted between the base electrode and the octagon upper side.

3.2 Tested mechanical displacements



The equivalent capacitance C_i is roughly inversely proportional to the mechanical gap g_i between the 2 correspondent electrodes tips:

$$dC_i/C \propto -dg_i/g.$$

In order to test the good relation between g_i and C_i , different mechanical

displacements of the upper electrode have been realized:

- Since g_3 and g_4 do not vary, C_3 and C_4 must be kept constant.
- C_1 and C_2 are expected to increase (\uparrow) or decrease (\downarrow) depending on the motion direction (Table 1).

Table 1: Tested displacements

	"V" Vertical translation (dX=0, dY>0)	"H" Horizontal translation	
		Q2 \Rightarrow Q1 (dX < 0, dY=0)	Q1 \Rightarrow Q2 (dX > 0, dY=0)
C_1	\downarrow	\uparrow	\downarrow
C_2	\downarrow	\downarrow	\uparrow
C_3	\approx constant	\approx constant	\approx constant
C_4	\approx constant	\approx constant	\approx constant

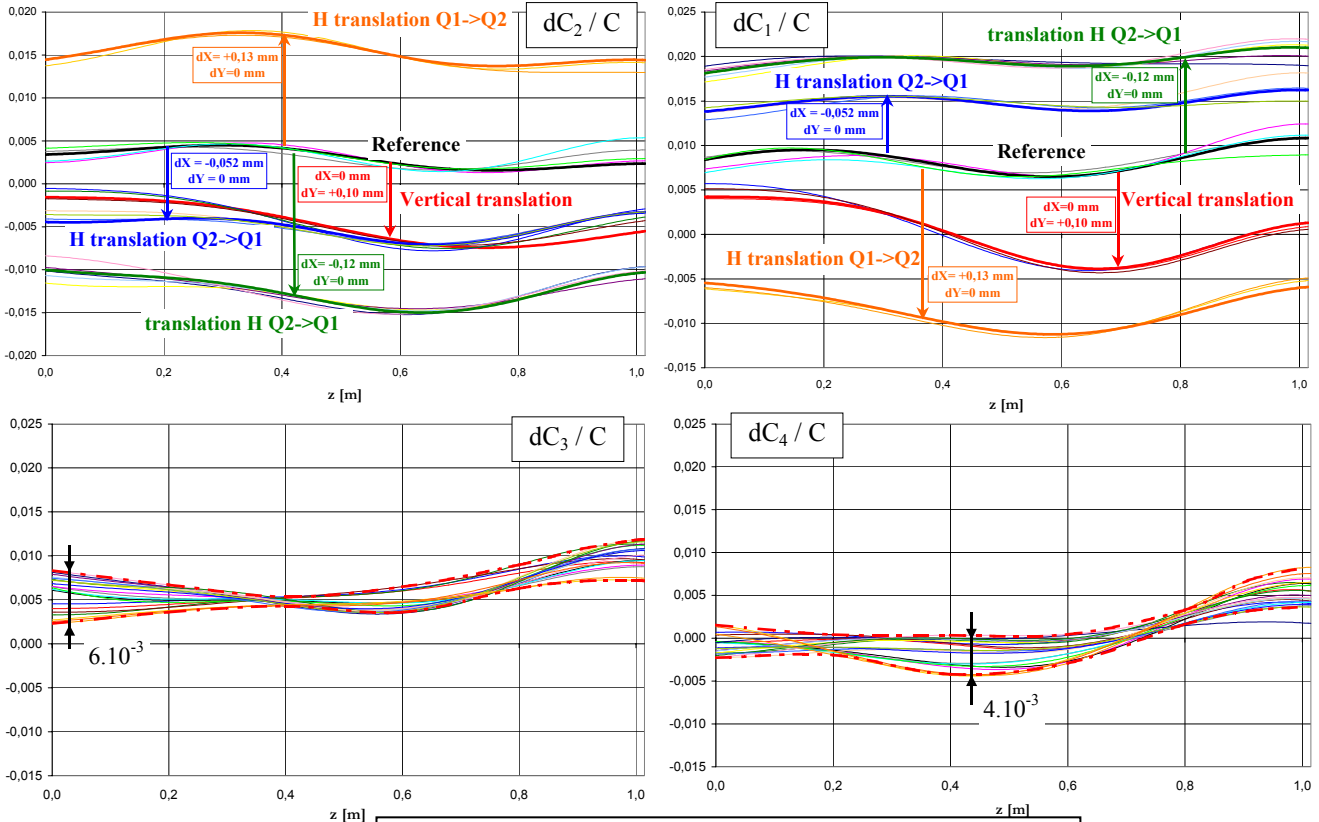


Fig. 3: capacitance variations vs. different tested translations

3.3 Results

- The superimposition of the capacitance profiles estimated from the several field measurements made for each displacement shows a very good reproducibility.
- The signs of the estimated dC_1/C and dC_2/C perfectly agree with the direction of the translation. For example, when the electrode is horizontally displaced towards Q_1 by $dx=-0,052$ mm, g_1 decreases while g_2 increases. Indeed $dC_1/C \propto -dg_1/g > 0$ and $dC_2/C \propto -dg_2/g < 0$.
- The tested vertical translation has indeed been diagnosed by a simultaneous decrease of dC_1/C and dC_2/C .
- The capacitance default estimation is proportional to the amplitude of the mechanical shift. The capacitance default estimated for the 0,12 mm H translation is twice greater than the dC/C computed for the 0,052 mm H translation. So this diagnosis gives a quantitative information.
- As expected, whatever displacement is realised, C_3 and C_4 are constant. The maximum dispersion of these estimations derived from 12 bead-pull measurements is of the order of $5 \cdot 10^{-3}$. Compared to the smallest tested translation, this dispersion implies that the limit of this RF diagnosis would be reached for a 20 μ m translation.

4 VALIDATION OF END BOUNDARY INDEPENDENCE

The modularity of the cold-model permits to mount different sets of pieces depending on the end region to be configured:

- Pieces with undercut, designed to be screwed at the ends of the vanes, and dedicated plates form an input- output- or coupling-cell;
- Short vane elements can be added to assemble electrodes longer than 1 body length.

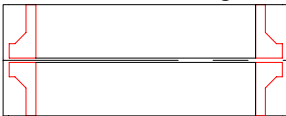


Fig. 4: 1-m long RFQ

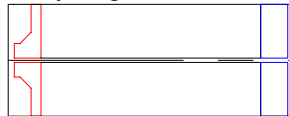


Fig. 5: 1-end detuned RFQ

For the study of the end region independence of our RF estimations, two different configurations of 1-m long RFQ have been tested:

Conf. #1- The 2 end regions are terminated with matched undercuts (Fig. 4)

Conf. #2- One of the end pieces has been replaced by a short vane element (Fig. 5 and 6). A cylindrical cap is mounted on the flange to isolate RF measurements from outside perturbations (Fig. 7).



Fig. 6: abrupt ending



Fig. 7: cylindrical cap at the end

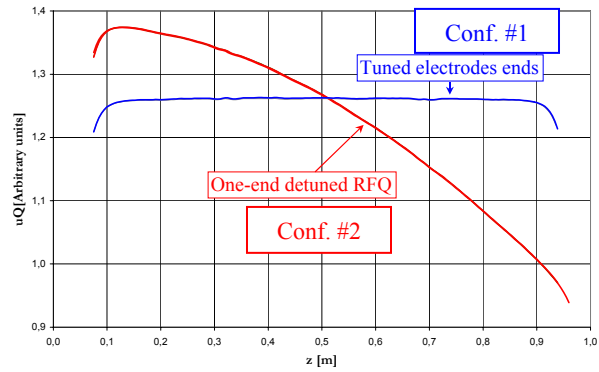


Fig. 8: uQ profile

The longitudinal distribution of the quadrupole component $uQ(z)$ of the accelerating mode (Fig. 8) is constant with the matched ends. The abrupt ending piece detunes the end boundary conditions: the profile of $uQ(z)$ slopes down steeply.

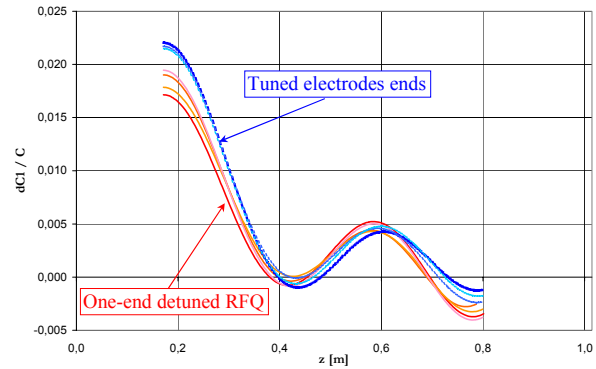


Fig. 9: dC_1 estimated in the 2 configurations

The profiles of the estimated defaults are very close whenever the end region is matched or not (Fig. 9). The end detuning is largely compensated. It validates the independence of the central region default estimation from the boundary conditions.

5 CONCLUSION

Experimental tests show a good correlation between mechanical defaults and our RF estimations whatever the end boundary conditions are. Translations of the electrodes as small as 20 μ m can be detected. Though being less precise than 3d mechanical measurement probes, this diagnosis is very relevant since it can be applied inside the cavity even after its brazing.

Each individual RFQ segment of the IPHI RFQ will be tested before and after brazing. Any relative displacements of the 4 segment pieces on the brazing surfaces will be checked.

6 REFERENCES

- [1] F. Simoens, A. France, "Theoretical Analysis of a Real-life RFQ Using a 4-Wire Line Model and the Spectral Theory of Differential Operators.", this conference (EPAC2002, Paris).